AIP | The Journal of Chemical Physics

The spin and orbital contributions to the total magnetic moments of free Fe, Co, and Ni clusters

Jennifer Meyer, Matthias Tombers, Christoph van Wüllen, Gereon Niedner-Schatteburg, Sergey Peredkov, Wolfgang Eberhardt, Matthias Neeb, Steffen Palutke, Michael Martins, and Wilfried Wurth

Citation: The Journal of Chemical Physics **143**, 104302 (2015); doi: 10.1063/1.4929482
View online: http://dx.doi.org/10.1063/1.4929482
View Table of Contents: http://scitation.aip.org/content/aip/journal/jcp/143/10?ver=pdfcov
Published by the AIP Publishing

The spin and orbital contributions to the total magnetic moments of free Fe, Co, and Ni clusters

Jennifer Meyer,[1,a)] Matthias Tombers,[1] Christoph van Wüllen,[1]
Gereon Niedner-Schatteburg,[1,b)] Sergey Peredkov,[2,c)] Wolfgang Eberhardt,[2]
Matthias Neeb,[3] Steffen Palutke,[4] Michael Martins,[4] and Wilfried Wurth[4]
[1]*Fachbereich Chemie and Forschungszentrum OPTIMAS, Technische Universität Kaiserslautern, 67663 Kaiserslautern, Germany*
[2]*Institut für Optik und Atomare Physik, Technische Universität Berlin, Hardenbergstrasse 36, 10623 Berlin, Germany and DESY-CFEL, Notkestr. 85, 22607 Hamburg, Germany*
[3]*Helmholtz-Zentrum für Materialien und Energie, BESSY II, Albert-Einstein-Strasse 15, 12489 Berlin, Germany*
[4]*Institut für Experimentalphysik, Universität Hamburg, Luruper Chausee 149, 22761 Hamburg, Germany*

(Received 9 February 2015; accepted 12 August 2015; published online 8 September 2015)

We present size dependent spin and orbital magnetic moments of cobalt (Co_n^+, $8 \le n \le 22$), iron (Fe_n^+, $7 \le n \le 17$), and nickel cluster (Ni_n^+, $7 \le n \le 17$) cations as obtained by X-ray magnetic circular dichroism (XMCD) spectroscopy of isolated clusters in the gas phase. The spin and orbital magnetic moments range between the corresponding atomic and bulk values in all three cases. We compare our findings to previous XMCD data, Stern-Gerlach data, and computational results. We discuss the application of scaling laws to the size dependent evolution of the spin and orbital magnetic moments per atom in the clusters. We find a spin scaling law "per cluster diameter," $\sim n^{-1/3}$, that interpolates between known atomic and bulk values. In remarkable contrast, the orbital moments do likewise only if the atomic asymptote is exempt. A concept of "primary" and "secondary" (induced) orbital moments is invoked for interpretation. © *2015 AIP Publishing LLC*. [http://dx.doi.org/10.1063/1.4929482]

I. INTRODUCTION

The discussion of magnetic phenomena in homogeneous samples of bulk materials focuses on the dominant exchange coupling of localized spins at atomic centers. The concomitant orbital angular moments of individual electrons quench in the bulk due to orbital hybridization and symmetry reduction. Some orbital angular moments however persist in part. This gives rise to the adjustable bulk g-factors by, e.g., 4%–10% (Table I) corrections to the spin only g-factor (2.0) in the case of ferromagnetic 3d bulk metals. In the free atoms or ions of those metals, however, the spin and the orbital moments possess values of equal magnitude, e.g., the orbital moment of a free nickel atom even exceeds its spin moment. A change in system size obviously induces a change in the electronic structure which may manifest in a change of magnetic properties.

The evolution of magnetism with sample size and its application has been at the scientific focus for some time.[1,2] Size selected clusters became favorable objects to follow such evolution.[3–5] Suitable gas phase isolation experiments aim at the determination of intrinsic magnetic moments without the interference of either a supporting surface or of any other environment.[6] Stern-Gerlach (SG) experiments serve to determine the total magnetic moments of isolated transition metal clusters in the gas phase as shown by de Heer *et al.*[7] and others.[8–11] These experiments revealed enhanced magnetic moments compared to the bulk attributed to an enhanced contribution of the orbital magnetic moment. However, Stern-Gerlach experiments (see Sec. III D) conceptually lack the capability to separate the magnetic moment into its spin and orbital contributions. Moreover, the *ab initio* description of the orbital magnetic moment is still a challenge, despite the ongoing progress in the field (see Sec. III E).[12] Problems arise from the highly correlated nature of the magnetic materials.

X-ray magnetic circular dichroism (XMCD) spectroscopy has proven instrumental to elucidate the spin and orbital contributions to total magnetic moments of bulk samples.[13–15] Enhanced orbital moments were found in low-dimensional samples, e.g., thin films,[16,17] nano structures,[18,19] deposited clusters,[4,20,21] or adatoms.[22,23] Recently, it became feasible to conduct XMCD spectroscopy of highly diluted samples in the gas phase.[24–26] Accordingly, it was expected to find an enhancement with respect to the bulk of orbital magnetic moments in isolated clusters. Indeed, the findings of both contemporary gas phase experimental setups[24–26] have revealed orbital magnetic moments of clusters that are quenched with respect to the atomic values, but enhanced with respect to the bulk. The differences in the spin magnetic moments are less pronounced.

A question arises when investigating cluster properties is the following: Does every atom count as in the so called

a)Present address: Institute for Ion Physics and Applied Physics, Universität Innsbruck, Technikerstr. 25, 6020 Innsbruck, Austria.
b)Author to whom correspondence should be addressed. Electronic mail: gns@chemie.uni-kl.de
c)Present address: Max-Planck-Institut für Chemische Energiekonversion, Stiftstr. 34-36, D-45470 Mülheim an der Ruhr, Germany.

TABLE I. Magnetic moments of the atom, cluster, and bulk for iron, cobalt, and nickel in comparison with spin orbit coupling (SOC) constants for the atom/ion and g-factors for the bulk. Relationship between the different g-factors and g′ is given in the Appendix.

	Magnetic moment (μ_B/atom)			Landé	g′	g-	
	Orbit	Spin	Total	g-factor	factor	factor	SOC constant (cm^{-1})
Fe_1[a] ^5D $[Ar]4s^23d^6$	2	4	6	1.50			−104[b]
Fe_1^+[a] ^6D $[Ar]4s^13d^6$	2	5	7	1.71			−86[c]
Fe_n^+[d]	0.24	2.82	3.07	1.85		2.18	
Fe (bcc, bulk)[e]	0.083	1.98	2.063		1.92[f]	2.09[g]	
Co_1 ^4F $[Ar]4s^23d^7$	3	3	6	1.33			−181[h]
Co_1^+ ^3F $[Ar]4s^03d^8$	3	2	5	1.40			−238[i]
Co_n^+	0.55	2.28	2.83	1.68		2.49	
Co (hcp, bulk)[e]	0.153	1.55	1.703		1.84[j]	2.25[g]	
Ni_1 ^3F $[Ar]4s^23d^8$	3	2	5	1.25			−333[k]
Ni_1^+ ^2D $[Ar]4s^03d^9$	2	1	3	1.33			−603[c]
Ni_n^+	0.33	1.42	1.75	1.68		2.49	
Ni (fcc, bulk)[l]	0.06	0.6	0.66		1.84[m]	2.18[g]	

[a]Magnetic moments for atoms and cations calculated according to Hund's rules.
[b]Spin orbit coupling (SOC) constants extracted by Landé interval rule form experimental values: Refs. 98 and 99.
[c]Spin orbit coupling (SOC) constants extracted by Landé interval rule form experimental values: Refs. 99 and 100.
[d]Average moments of the measured size range of Fe_n^+, Co_n^+, and Ni_n^+, this work.
[e]Magnetic moments from Ref. 14.
[f]Magnetomechanical ratio g′: Ref. 95.
[g]Taken from Ref. 7.
[h]Spin orbit coupling (SOC) constants extracted by Landé interval rule form experimental values: Refs. 99 and 101.
[i]Spin orbit coupling (SOC) constants extracted by Landé interval rule form experimental values: Refs. 99 and 102.
[j]Magnetomechanical ratio g′: Ref. 96.
[k]Spin orbit coupling (SOC) constants extracted by Landé interval rule form experimental values: Refs. 99 and 103.
[l]Magnetic moments from Refs. 49 and 50.
[m]Magnetomechanical ratio g′: Ref. 97.

"non-scalable" size regime or will a trend be followed from the bulk to the atomic value? For large cluster sizes, the properties follow a scaling law which interpolates between the bulk and the atomic values (Table I). Once the "non-scalable" size regime is reached, individual fluctuations are superimposed onto the general trend. There may be noticeable changes in the recorded magnetic moments if one adds or subtracts an atom to a given cluster. Electronic and/or geometric shell closures might occur as well.[12] Therefore, we analyzed the cluster size dependence of spin and orbital magnetic moments for conceivable scaling laws. We have found that the general trend of the spin and orbital magnetic moments each follows a different scaling law which was not to be expected. Individual cluster sizes reveal magnetic moments that are enhanced or diminished with respect to the scaling law values. These are the non-scalable fluctuations that superimpose. Implications of this behavior will be discussed in Sec. V.

The paper is organized as follows: we introduce the applied combination of experimental techniques and explain the XMCD data evaluation scheme. Subsequently, we present the recorded XMCD data and discuss the obtained spin and orbital moments of iron, cobalt, and nickel cluster cations. Next, we compare our total magnetic moments to prior data from Stern-Gerlach experiments and we compare to spin only moments by computations. A dedicated chapter on concepts of scaling laws precedes our final conclusions. We collect extra material in Appendices A and B and in the supplementary material.[118]

II. EXPERIMENTAL METHODS AND DATA EVALUATION SCHEME

A. The experimental setup for XMCD data recording

The experimental setup ("GAMBIT") consists of a modified Fourier Transform-Ion Cyclotron Resonance (FT-ICR; Apex IV, Bruker Daltonics) mass spectrometer which was coupled to a soft X-ray undulator beamline at the Helmholtz-Zentrum Berlin / BESSY II (UE52-PGM) as described before.[24,27] A cryogenic cooling of the ICR cell to 20 K is enabled through an extensive modification of the ICR cell housing. Metal clusters on choice are generated by a custom laser vaporization cluster ion source.[28,29] This source utilizes a Q-switched Nd:YAG laser (532 nm, 20 Hz) which is focussed onto the metal target to ablate atomic matter into a short transverse helium gas pulse which yields clusters by swift aggregation. A homebuilt piezoelectric valve provides for the gas pulse.[30] Mono isotopic target materials were used in the case of iron (Oak Ridge National Laboratory, Fe-56, 99.93%) and nickel (Oak Ridge National Laboratory, Ni-58, 99.61%) in order to avoid multi isotopic dilution of the signal intensity. The cluster ion beam is transferred into the ICR cell which serves as ion trap as well as mass analyzer. The desired cluster size is selected, isolated, and buffer gas cooled to an appropriately low temperature ($T \leq 20$ K). The superconducting magnet ($B = 7$ T) of the FT-ICR aligns the magnetic moments of the cluster ions. X-ray absorption spectra (XAS) were measured in Total Ion Yield (TIY), i.e., the trapped cluster ions are

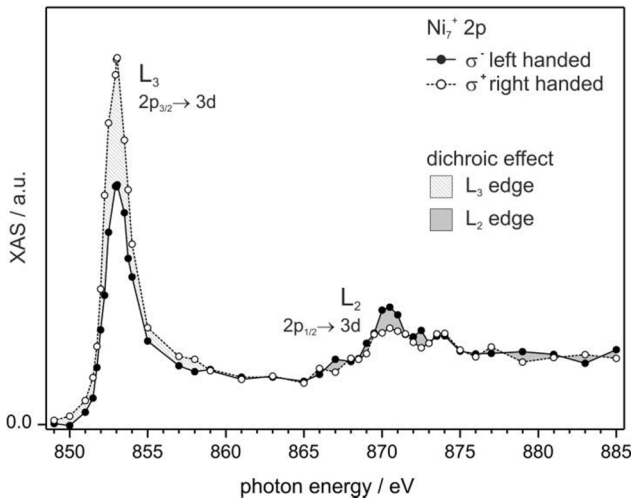

FIG. 1. Polarization dependent X-ray absorption spectra for Ni_{12}^+ at the $L_{2,3}$ edge. The spectra were recorded with negative (open symbols) and positive (filled symbols) circular photon polarizations with the propagation direction of the X-ray beam parallel to the magnetic field axis. Shaded areas indicate the X-ray magnetic circular dichroism (XMCD) effects for the L_2 and L_3 edges. Spin and orbital magnetic moments are extracted following the procedure outlined by Chen *et al.*[14]

exposed to the X-ray beam and the subsequent fragmentation is measured. We recorded fragmentation mass spectra while tuning the photon energy. By summation of all fragment intensities and subsequent normalization to the X-ray photon flux and to the parent cluster intensity, we obtain an integrated and normalized fragmentation spectrum that is equivalent to a relative XAS. We obtained L-edge XMCD spectra by subtraction of XAS for both photon helicities (left- and right-handed polarization, lcp and rcp; 90% polarization at beamline UE52-PGM), cf. the example of Ni_7^+ in Fig. 1. Clearly resolved dichroic effects are visible at both the L_2 and the L_3 edges. We obtained XMCD spectra for cobalt, iron, and nickel cluster cations in the size range of seven to twenty atoms per cluster. We account for the finite degree of X-ray polarization throughout the further data evaluation.

B. The XMCD data evaluation scheme

The projections of the clusters' spin and orbital magnetic moments upon the quantization axis are extracted from the spectra by magneto-optical sum rule analysis.[14,31,32] The z axis, as quantization axis, coincides with the magnetic field axis of the ICR magnet. The magnetic field axis is collinear with the propagation direction of the X-ray beam. We obtain the numerical values of the z components of spin- and orbital moments, $m_S^{(z)}$ and $m_L^{(z)}$[14] in units of μ_B, by the customized sum rule evaluation formulas,

$$m_L^{(z)} = \left[-\frac{4\,(A+B)}{3C} n_h\right] / \eta_{pol}, \qquad (1)$$

$$m_S^{(z)} = \left[-\frac{2\,(A-2B)}{C} n_h - 7\,\langle T_z\rangle\right] / \eta_{pol}. \qquad (2)$$

The parameters **A** and **B** represent the integrated dichroic effects ($\sigma^+ - \sigma^-$) at the L_2 and L_3 absorption edges of the experimental spectra (Fig. 1). **C** is the corresponding value of the isotropic spectrum which is approximated by the sum of spectra of both polarizations ($\sigma^+ + \sigma^-$), corrected for non-resonant background absorption.[14] $\langle T_z\rangle$ is the anisotropic dipole term, and n_h is the number of unoccupied 3d valence states per atom ("3d holes"). The finite degree of circular polarization η_{pol} (in present case: 90%) necessitates the application of an according linear correction.

There are clear relations amongst the number of 3d holes n_h, the number of unpaired electrons $5 - |5 - n_h|$, the total spin $S = 1/2(5 - |5 - n_h|)$, and the spin magnetic moments per atom $m_S = (5 - |5 - n_h|)\ \mu_B$. The $4s^2 3d^x$ configurations of Fe, Co, and Ni atoms (x = 6, 7, 8) thus determine via $n_h = 4$, 3, and 2 their spin magnetic moments $m_S = 4\ \mu_B$, 3 μ_B, and 2 μ_B. In the bulk phase, the diffuse 4s atomic orbitals form a broad conduction band, whereas the compact 3d orbitals are less overlapping and form a narrower valence band. As a result, the conduction (4s) band is more or less half-filled and the spins are paired to a large extent. The 3d population is then substantially increased. The value of 3d holes n_h reduces in the bulk with respect to atomic samples. Possible issues on the determination of bulk n_h values have been discussed before.[33] Currently accepted values of bulk phase 3d holes per atom are $n_h^{bulk} = 3.4$[34,35] for iron, $n_h^{bulk} = 2.5$[14] for cobalt, and $n_h^{bulk} = 1.45$[36,37] for nickel. Most recently, an independent study[26] elaborately concluded in $n_h(Fe) = 3.3 \pm 0.2$, $n_h(Co) = 2.5 \pm 0.2$, and $n_h(Ni) = 1.3 \pm 0.2$. Both sets of values agree within stated uncertainties to better than 3%. For the purpose of the current study, we chose to utilize the former set of n_h data.

Small clusters are single domain particles[38,39] which can be considered to behave super paramagnetic.[40–42] The magnitudes of XMCD spin magnetic moments per atom m_s are expected to range around the superparamagnetic prediction of $m_s^{(sp)} = n_e^{(u)} s\, g_e\, \mu_B = n_h^{bulk} s\, g_e\, \mu_B$, where $n_e^{(u)}$ is the number of unpaired electrons per atom, and s and g_e indicate the electron spin and its gyromagnetic ratio. The latter equality holds in the case of elements with more than half filled valence sub shells. Deviations of the recorded XMCD spin magnetic moments from the predicted $m_s^{(sp)}$ values indicate electronic rearrangement within the clusters with respect to the corresponding bulk material. The documentation of recorded XMCD spin magnetic moments (Fig. 2) includes the above cited n_h values for ease of comparison.

The anisotropic dipole term in Eq. (2), $\langle T_z\rangle$, treats a possible anisotropy in the spin distribution of the investigated sample. It corresponds to a spin asymmetry along the quantization axis. It may modulate the spin magnetic moment in a highly anisotropic medium up to 20%,[43] and it would cancel by an angular average.[44] A previous XMCD experiment has verified the absence of linear dichroism in an iron cluster, i.e., Fe_{10}^+, when stored as isolated ions within an ion trap.[26] This provides for an experimental verification that $\langle T_z\rangle$ is small enough to allow for a decoupling of the spin magnetic moment from the clusters nuclear framework. Thus, at the current field strength (7 T), the magnetic moments of the cluster may align (see below), while the cluster body - its framework of nuclei - is able to rotate freely. At any time, their nuclear orientation is random. In the following, we approximate $\langle T_z\rangle \approx 0$. The opposite case, $\langle T_z\rangle \neq 0$, would imply that magnetic moments do not rotate independently of the cluster nuclear framework.

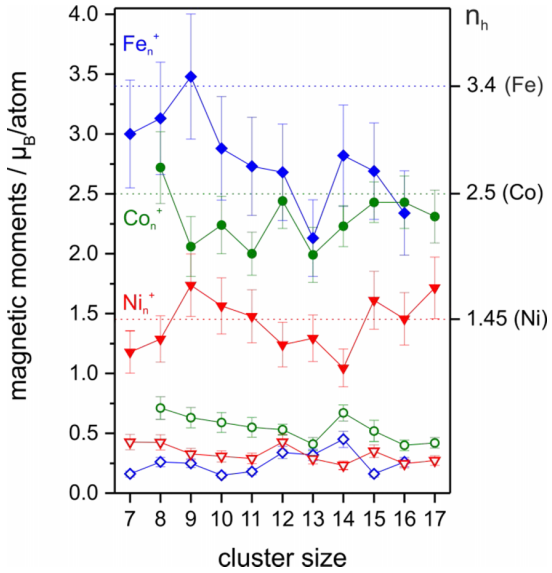

FIG. 2. Spin (filled symbols) and orbital (open symbols) magnetic moments of iron Fe_n^+ (diamonds), cobalt Co_n^+ (circles), and nickel Ni_n^+ (triangles) cluster cations. Dashed lines indicate the number of 3d holes as used in the evaluation of the spin and orbital magnetic moments (see Sec. II B XMCD data evaluation scheme).

Then, the magnetic crystalline anisotropy energy would exceed the thermal rotational energy. The magnetic moments would lock to the cluster frame below a critical blocking temperature, in short a locked moment behavior.

The projection of quantized magnetic moments upon a quantization axis obeys the Brillouin function $f_{Br}(T, B)$ in dependence of sample temperature T and external magnetic field strength B.[45] It is well approximated by the classical Langevin function $f_{La}(T, B)$.[9,41,46,47] Thus, the projections of the magnetic moments onto the quantization axis are functions of cluster temperature and applied magnetic field. The intrinsic spin magnetic moments m_S and the intrinsic orbital magnetic moments m_L derive from their measured projections $m_S^{(z)}$ and $m_L^{(z)}$. The intrinsic magnetic moments would correspond to a sample magnetization at 0 K and infinite magnetic field. In the present case of 3d metal clusters, the experimental conditions ($T_{cluster}$ = 20 K and $B_{external}$ = 7 T) indicate Russel-Saunders (LS) coupling, and it is the total magnetic moment which aligns to the external magnetic field.[25] Note that our previous study has considered both LS coupled and Paschen-Back decoupled magnetic moments.[24]

Deriving the spin and orbital magnetic moments by sum rule analysis is known to imply a systematical error of ±5%–10%.[48] Further uncertainty enters by the choice of n_h, by the choice of the integration regions, and by the subtraction of nonresonant background. Some minor uncertainty arises through the indirect knowledge of cluster temperature which enters into the Langevin scaling. We estimate these parameters to add another ±5% uncertainty. In total, we derive an uncertainty of our spin and orbital magnetic moments of ±15% (1σ standard deviation).

III. RESULTS AND DISCUSSION

The spin and orbital magnetic moments of small iron, cobalt, and nickel cluster cations, Fe_n^+, Co_n^+, and Ni_n^+, were measured under the same experimental conditions as our previously published data on some cobalt clusters.[24]

A. Magnetic moments of iron clusters by XMCD

We investigated iron cluster cations Fe_n^+ in the size range from 7 ≤ n ≤ 16 and n = 18 atoms per cluster. The spin magnetic moments range from 2.13 ± 0.3 to 3.48 ± 0.47 μ_B/atom and the orbital magnetic moments range from 0.45 ± 0.07 to 0.12 ± 0.02 μ_B/atom (Fig. 2). Spin and orbital magnetic moments are enhanced with respect to the bulk values (Fe, bcc) of m_S = 1.98 μ_B/atom and m_L = 0.083 μ_B/atom.[14] This enhancement of spin magnetic moments (factor 1.1–1.8) is smaller than that of the orbital magnetic moments (factor 1.5–4.0). Both the spin and the orbital magnetic moments of the clusters are significantly quenched with respect to their atomic values (cf. Table I).

The cluster size dependent absolute variations of spin moments in iron clusters are larger than those of the orbital moments, relative variations are comparable. Our spin magnetic moment of Fe_{13}^+ (2.13 ± 0.3 μ_B/atom) is the smallest of all those measured in agreement with the work of Lau *et al.*[25] who found an interpretation in terms of an antiferromagnetic coupling in conjunction with icosahedral geometric shell closure in the case of this particular cluster size. Our spin magnetic moments of Fe_{15}^+ and of Fe_{16}^+ (2.7 ± 0.4 and 2.30 ± 0.35) are smaller than those reported by Lau *et al.* (3.7 ± 0.5 and 3.7 ± 0.5). The recorded deviations of both data sets range slightly beyond the combined uncertainties. For sure, these deviations are minor as compared to the significant reduction of spin magnetic moment in Fe_{13}^+, where both data sets agree well.

Our experimental spin magnetic moments of Fe_n^+ clusters are on the average lower by 10% than the average of the previously reported ones.[25] This difference is not explained by the different choice of n_h values which by themselves differ by 3% (cf. Sec. II).

The orbital magnetic moments of our present study agree very well with those of Lau *et al.*[25] in the case of nine cluster sizes (Fig. S2).[118] In two cases, the agreement is inferior: our value for Fe_{14}^+ (0.45 ± 0.07 μ_B/atom) is higher than theirs (0.14 ± 0.35 μ_B/atom), while their value for Fe_9^+ (0.6 ± 0.35 μ_B/atom) is higher than ours (0.25 ± 0.04 μ_B/atom). In all cases, however, there is an agreement within combined 1σ uncertainties.

B. Magnetic moments of cobalt clusters by XMCD

We have determined spin and orbital contributions to total magnetic moments of isolated cobalt clusters (Co_n^+, 8 ≤ n ≤ 17 and n = 19, 22) by the XMCD technique before,[24] and there has been an independent study on a limited cluster size range (n = 10–15).[26] Here, we report on a novel data set that originates from a re-evaluation of our previous experimental recordings. In all cases, our new and previous XMCD spectra agree reproducibly well to within less than 10% deviation.

The current spin magnetic moments of the clusters are larger than the bulk value by approximately 1 μ_B per atom (cf. Table I). Our spin magnetic moments are lower than those of Lau *et al.*[26] with a minimum deviation of 1% for Co_{15}^+ and a maximum deviation of 20% for Co_{13}^+ (Fig. 2; n = 19, 22 in Tables S3a and S3b[118] and Fig. S2;[118] see also Figs. 3 and 4).

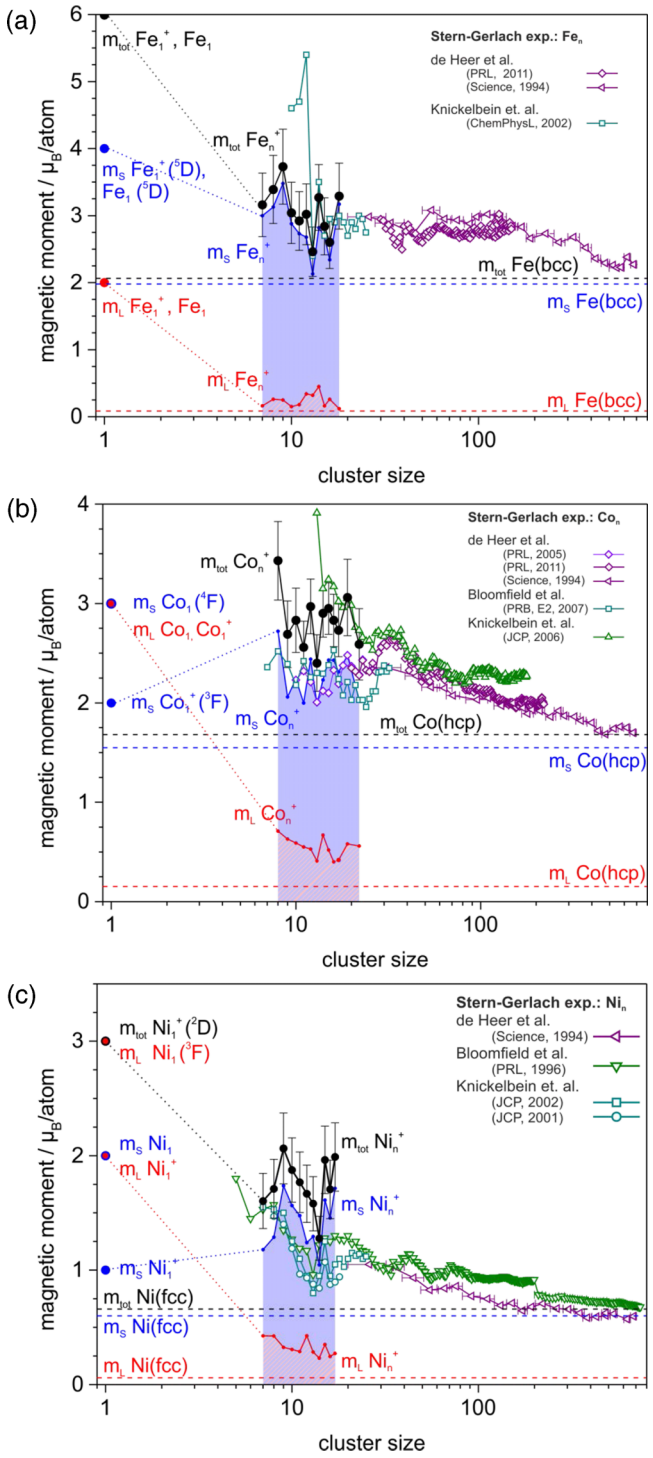

FIG. 3. Total Magnetic moments (filled circles) determined by XMCD experiments in comparison with Stern-Gerlach results (open symbols). (a) Fe_n^+, (b) Co_n^+, and (c) Ni_n^+. Shaded areas indicate the spin (solid, blue) and orbital (hatched, red) magnetic moments. Dashed lines display the magnetic moments of the respective bulk material (Fe and Co[14] and Ni[49,50]). The magnetic moments of the free atom and cation were calculated according to Hund's rules. Stern-Gerlach results were taken from Refs. 7, 51, and 55 for Fe_n^+, from Refs. 7 and 51–54 for Co_n^+, and from Refs. 7 and 9–11 for Ni_n^+. For Ref. 51, the magnetic moments for the assigned high spin states are plotted and for Ref. 52, the experimental series denoted E2 is plotted. The Stern-Gerlach experiments investigated a wide cluster size range of up to several hundred atoms per clusters. The magnetic moment does not smoothly approach the bulk value with increasing cluster size but shows an oscillatory behavior. These oscillations are due to electronic and/or geometric shell closures and are superimposed onto the general trend.[12] Our narrow size range does not allow us to detect these oscillations.

Except for the Co_{13}^+ cluster, spin magnetic moments agree within combined experimental uncertainties.

The orbital magnetic moments reveal almost constant values of about 0.55 ± 0.05 μ_B/atom. Note that the present experiments cover a wider range of cluster sizes than the experiments in Ref. 26. The orbital moments vary between 0.4 and 0.7 μ_B/atom within our investigated cluster size range. This corresponds to a quenching of the atomic value of 3 μ_B or to an enhancement by a factor of 2–4 of the bulk value (m_L (Co, hcp) = 0.153 μ_B/atom[14]).

C. Magnetic moments of nickel clusters by XMCD

By virtue of the present study, we achieve an extension in size range with respect to previously published XMCD data on the spin and orbital magnetic moments of nickel clusters Ni_n^+ (n = 10–15).[26] Our XMCD data set covers the extended range of n = 7–17. We find very good agreement of both data sets within the overlapping size range, the previous spin magnetic moments being 10%–20% lower than our new values, which falls within the combined uncertainties.

We find considerable fluctuations of spin magnetic moments throughout our investigated size range: they range from 1.05 ± 0.1 μ_B/atom for Ni_{14}^+ to 1.74 ± 0.2 μ_B/atom for Ni_9^+. They are quenched with respect to those of isolated atoms (2 μ_B/atom in Ni [Ar]$4s^2 3d^8$, ^{3}F), and they are enhanced with respect to those of the bulk (Ni (fcc), 0.6 μ_B/atom[49,50]).

There is very good agreement of the present nickel data set with the previously published data[26] on the magnitudes of the orbital magnetic moments within the overlapping cluster size range (cf. Fig. S2 in the supplementary material).[118] Cluster size dependent variations are minor (±25%) and smooth.

The orbital magnetic moments of small nickel cluster cations ($7 \le Ni_n^+ \le 17$) range from 0.25 to 0.43 μ_B/atom, and they are enhanced with respect to those of the bulk (Ni (fcc), 0.06 μ_B/atom[49,50]). They are quenched with respect to those of isolated atoms (3 μ_B/atom in Ni [Ar]$4s^2 3d^8$ ^{3}F). The orbital moment of Ni_{12}^+ is enhanced by 0.14 μ_B/atom with respect to the neighboring cluster sizes (cf. Fig. 2).

Both of our data sets, on the spin magnetic moments of cobalt and iron clusters, provide for slightly smaller values than those of Lau *et al.* Our data on the spin magnetic moments of nickel clusters, however, reveal slightly larger values than those of Lau *et al.* as discussed above. Neither of both experiments suffered from major variation of experimental parameters. Thus, it is conclusive to interpret the recorded small differences as within statistical variations. We thus conclude on a verification of spin and orbital magnetic moments through two independent studies (present and previous) which have revealed values that mostly agree within combined error bars. The magnitudes of these magnetic moments thereby become known and confirmed entities that may compare to related cluster properties as obtained by other methods.

D. XMCD data on cationic clusters and Stern-Gerlach data on neutral clusters

Gas phase XMCD experiments determine partial magnetic moments of cationic clusters; SG experiments determine total magnetic moments (SG moments) of neutral clusters.

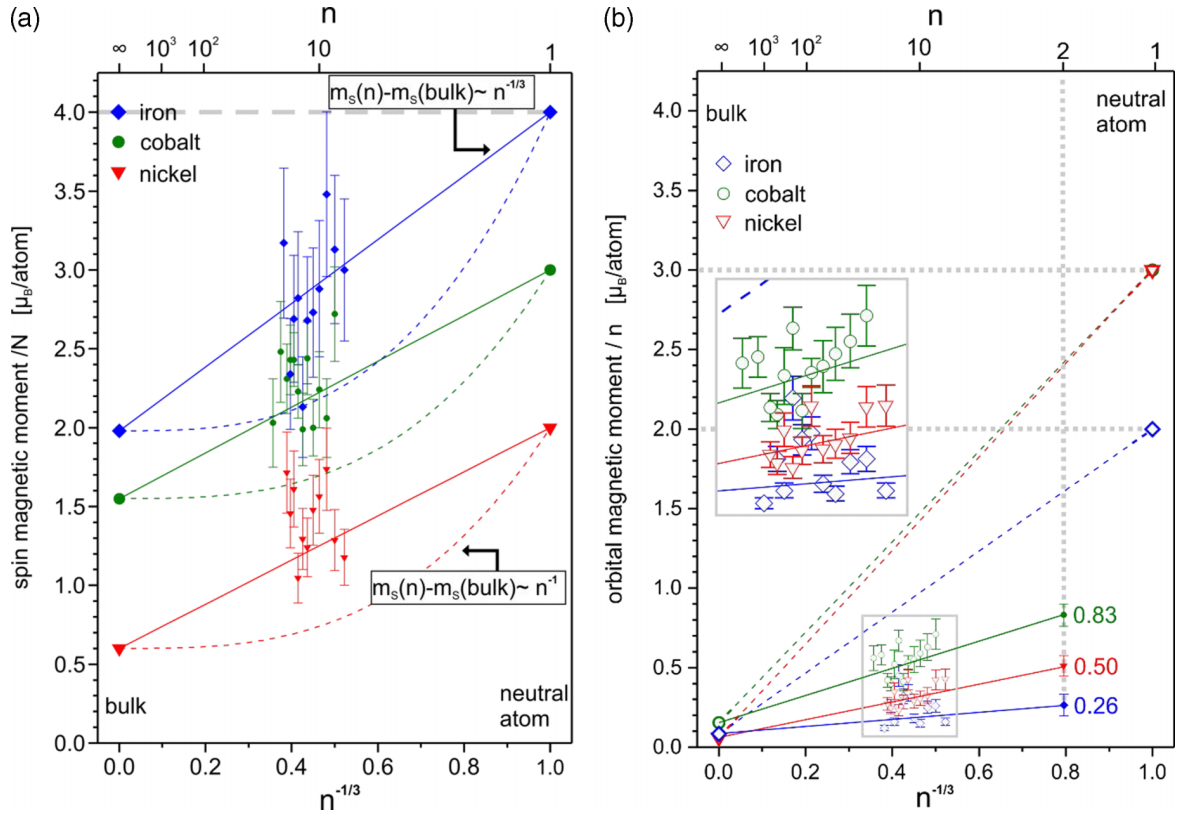

FIG. 4. Spin (left) and orbital (right) magnetic moments of size selected clusters in comparison to conceivable trends that would interpolate between bulk metals and neutral atoms. Note that the recorded spin moments seem to follow an $n^{-1/3}$ scaling. Orbital moments of n = 2 clusters ($n^{-1/3} = 0.794$, solid symbols) are tentative predictions from the $n^{-1/3}$ fits of experimental bulk and cluster data as displayed with atomic values exempt from the fit.

Partial XMCD moments due to spin and orbital contributions add up to total magnetic moments (XMCD moments). Current gas phase XMCD experiments take place on samples after *in situ* equilibration by buffer gas cryo-cooling; SG experiments utilize supersonic expansion for irreversible cooling down to estimated temperatures. Current gas phase XMCD experiments utilize homogeneous magnetic fields of 5-7 T; SG experiments have utilized inhomogeneous magnetic fields of 1-2 T. Gas phase XMCD allows for orientation and relaxation of magnetic moments of the cluster samples on the time scale of multiple seconds in the presence of cold collision partners; previous SG experiments work on the microsecond time scale through relaxation of magnetic moments without collision partners. In summary, it is not obvious that magnetic measurements by the XMCD scheme and by the SG scheme compare well and would lead to identical data (Figs. 3(a)–3(c)).

The charge state of a cluster makes the less of a difference, the larger the cluster is. The positive charge of, e.g., Fe_8^+, Co_8^+, or Ni_8^+ cluster increases by one numerator and decreases by one denominator in the ratio of unoccupied to occupied valence states (3d, 4s) with respect to that of neutral clusters: 32/64, 24/72, or 16/80 (neutral) to 33/63, 25/71, or 17/79 (cationic), respectively. By virtue of the prevailing cases of more than half filled valence shells, the cationic clusters should bear total spin magnetic moments that should be larger by 1 μ_B than those of neutral clusters. Per cluster atom, this dilutes to small enhancements of 1/n μ_B, e.g., in the case of n = 8, the cationic charge makes up for an increase of 0.125 μ_B/atom in spin magnetic moment per atom. The ratio of vacant to occupied states (holes to electrons within the valence shell) increases through charging by mere 2% in Fe_{20}^+, while it increases considerably by 7.6% in Ni_8^+. We thus anticipate that cationic charge has little influence on magnetic moments (and geometry) of large iron clusters and probably some influence on small nickel clusters. The case of charges in cobalt clusters is intermediate. These estimates require consideration when comparing XMCD data and SG data with each other.

The magnitudes of total magnetic moments of cationic cobalt clusters by XMCD range amongst the considerable scatter of currently available Stern-Gerlach data.[7,51–54] The total magnetic moments deduced from the XMCD experiments are larger than the SG moments of de Heer *et al.*[7,51,54] and of Knickelbein,[53] and they are lower than those of Bloomfield *et al.*[52]

The total magnetic moments of the iron cluster cations by our current XMCD experiments reveal comparable magnitudes as obtained on neutral clusters by prior Stern-Gerlach experiments[7,51,55] for sizes n ≥ 13 (Fig. 3(a)). Our XMCD data of smaller clusters reveal little to no increase in magnitude (≤20%), while the SG moments of the sole available experiment jump in magnitude by a factor of two. This finding seems questionable to us - the more so as all but these data reveal a common trend of moderate variations by size.

Note that the exceptionally low XMCD moments of Fe_{13}^+ coincide with an exceptionally low SG moment of Fe_{13} - nicely supporting the antiferromagnetic coupling scheme within an icosahedral closed shell geometry[25] as discussed above and before.

The total magnetic moments of the neutral clusters (by Stern-Gerlach) and of cluster cations (by XMCD) of cobalt and iron show pronounced minima for the same cluster sizes, e.g., for Fe_{13}^+.[25,51,55] Our absolute values of the total magnetic moments by XMCD for cobalt and iron cluster cations are comparable to the values of neutral clusters by Stern-Gerlach experiments. Our total magnetic moment of the cationic nickel clusters by XMCD is larger by 40%–60% than that of neutral nickel clusters by Stern-Gerlach.[9–11] Note that the pattern of cluster size dependent variations in cationic nickel clusters resembles that of neutral nickel clusters but shifted by one atom—in contrast to the cases of cobalt and iron clusters where the significant reduction of total magnetic moments at n = 13 prevails for cations and neutrals alike. In the case of small nickel clusters, the charge state seems to influence magnetic moments significantly, whereas an according influence is not evident in the case of cobalt and iron clusters—much in line with the above discussed estimation.

Beyond the range of our present XMCD experiments, some of the Stern-Gerlach experiments have revealed repetitive oscillations in total magnetic moments of large clusters. These were interpreted convincingly in terms of a modulation by electronic and/or geometric shell closures.[7,12,56,57]

E. XMCD data in the light of previous computations

Density functional theory (DFT) served to obtain predictions for the spin magnetic moments of neutral iron clusters[58–65] and of cationic iron clusters,[33,58,66,67] of neutral cobalt clusters[59,64,67–75] and of cationic cobalt clusters,[67–69,76] and of neutral nickel clusters[47,59,64,67,68,77–80] and of cationic nickel clusters.[67,68,77] The predicted spin moments of the cationic clusters are smaller than the previous spin magnetic moments by XMCD experiments.[26] The found deviation was attributed to conceptual problems of approximate exchange-correlation functionals in describing highly correlated 3d electrons.

The published DFT predictions of spin magnetic moments of Fe_n^+ clusters in the size range from $7 \le n \le 20$[58,66] with a focus on Fe_{13}^+ [33,68,81] agree with the XMCD moments of the present study except on Fe_9^+ (XMCD experiment yields a larger spin magnetic moment) and Fe_{13}^+ and Fe_{16}^+ (XMCD experiment yields a smaller spin magnetic moment), cf. Fig. S4 in the supplementary material.[118] The exceptionally low spin magnetic moment found for Fe_{13}^+ has been interpreted in terms of an antiferromagnetic coupling of the center atom to its 12 surrounding surface atoms in an icosahedral geometry[25] with an ongoing controversy of its origin[33,81] prevailing. Our present XMCD spin magnetic moment of Fe_{13}^+ falls low by 0.5 μ_B/atom with respect to $Fe_{12,14}^+$ and thereby lends support to the idea of antiferromagnetic coupling in icosahedral geometry. The cited controversy could be solved in the future by application of the so far not yet applied broken symmetry approach to DFT calculations.[82,83]

The published DFT predictions of spin magnetic moments of Co_n^+ clusters in the size range from $2 \le n \le 30$[68,69,76] are lower than the XMCD moments of the present study except on $Co_{9,11,13}^+$ where perfect agreement is found, cf. Fig. S5 in the supplementary material.[118]

DFT treatments of Ni_{12} and Ni_{12}^+ conclude on icosahedral structures and yield predicted spin magnetic moments of 8 μ_B (0.67 μ_B/atom) and 9 μ_B (0.75 μ_B/atom), respectively,[68] which is significantly lower than the experimental value of 1.24 ± 0.2 μ_B/atom. In the case of the cationic cluster Ni_{13}^+ the same study obtained two almost degenerate isomers with spin magnetic moments of 0.69 μ_B/atom and 0.85 μ_B/atom, which is significantly smaller than the present spin magnetic moment by XMCD experiments of 1.3 ± 0.2 μ_B/atom. Another study covered an extended cluster size range for Ni_n^+ with $n \le 30$[77] and obtained spin magnetic moments that are about 0.3 μ_B/atom lower than those of the present XMCD experiments. The Ni_7^+ cluster constitutes an exception where the XMCD value of spin magnetic moment (1.2 μ_B/atom) agrees perfectly with the value from the above DFT study[77] and with those of another one.[67] Both studies conclude on a capped octahedron structure of Ni_7^+.

In conclusion, the present and previous XMCD experiments confirm the above theoretical predictions on quenching/enhancement of spin magnetic moments in small iron, cobalt, and nickel clusters with respect to atoms/the bulk. XMCD experiments and two dedicated model calculations[57,66] agree that the orbital magnetic moments in small iron and nickel clusters will be larger than the bulk values.[57,66] The particles' finite size leads to a reduced coordination number at the surface, such that the 3d electrons are more localized and therefore retain more of an orbital moment than the bulk does—much in line with previous discussion of magnetism in ultrathin films.[84] There will be size dependent shell closures modulating the actual values of the spin and orbital magnetic moments, superimposed on general trends.[7,12,56,57] The following discussion shall neglect such shell effects and elucidate the underlying, more general size dependent trends.

IV. SCALING LAWS OF THE SPIN AND ORBITAL CONTRIBUTIONS TO MAGNETIC MOMENTS OF Fe_n^+, Co_n^+, AND Ni_n^+ CLUSTERS?

Within the investigated size range, the obtained spin and orbital moments vary little. The values of the total magnetic moments fall within the range of those of previous investigations. Nevertheless, it pays to re-approach the data once more from a broad perspective. If clusters indeed interface between atom and bulk and if they truly bridge the gap in-between, one would expect a scaling of their properties by size. Such a scaling should interpolate between bulk properties and atomic properties and it should follow predictable trends when scaling from bulk to clusters. Reducing sizes further, one anticipates strongly size dependent and non-monotonous jumps in cluster features (as predicted and observed often before), which has led to the coinage of the term of a "non-scalable" size regime.[85,86] Note, however, that the scalability of properties is not obsolete. Instead, "magic cluster size" related variations superimpose onto the prevailing scaling laws (see Table II for various common scaling laws). In the present case of magnetic moments $m(n)$ and their individual contributions $m_x(n)$; $x = S, L$, conceivable scaling laws would read as follows:

$$m_x(n) = a_x + b_x n^{y_x}. \quad (3)$$

TABLE II. Various cluster properties and scaling laws–N refers to the number of particles or atoms per molecule or cluster.

Cluster property		Proportional to		
Surface tension of a spherical droplet	γ	$1/R^2$	=	$N^{-1/2}$
Ratio of surface to bulk atoms in a spherical particle	N_S/N_V	$1/R$	=	$N^{-1/3}$
Binding energy/atom (cohesive energy)[104–106]	ε_{coh}			$N^{-1/3}$
Ionization potential[107,108]	I_P			$N^{-1/3}$
Electron affinity[107,109]	E_a			$N^{-1/3}$
Resonance frequency of a spherical metal cluster[110–112]	ω_r	$1/R^3$	=	N^{-1}
Autoionization resonance energy of Hg clusters[113–115]	δ_n			N^{-1}
Average energy level spacing[116]	ΔE			N^{-1}
Magnetic dipolar interaction[117]	E_{mag}			N^{-1}
Cluster polarisabilities[112]	α_N	R^3		N

Note that these magnetic moments $m_x(n)$ refer to intensive values,[87] i.e., the magnetic moments are normalized "per atom." The parameters to determine are the reference values a_S and a_L, the scaling factors b_S and b_L, and the scaling powers y_S and y_L. The available experimental data of n = 7–17 would allow for a fit of these parameters—in principle. The concomitant uncertainties would render such a limited-size-range-fit meaningless, however. It is mandatory to consider the asymptotic limits and to evaluate physical models (Table II).

Assuming a cluster of n spherical atoms in dense packing and with total diameter L,[88] the cluster volume V_c scales to a good approximation as $V_c \sim n \sim L^3$. The number of surface atoms n_s goes by the surface area, $n_s \sim L^2$. The fraction of surface atoms n_S/n scales as $\frac{n_S}{n} \sim L^{-1} \sim n^{-1/3}$. This fraction of surface atoms may be a taken as a quantitative measure for the mixing in of atomic like magnetic properties, justified by the lower coordination of the surface atoms. Accordingly, y_x = −1/3, and an interpolation from the atomic case (all surface) to the bulk case (all volume) may read as

$$m_x(n) = a_x + b_x n^{-\frac{1}{3}}. \tag{4a}$$

In a second step, it may be assumed that $a_x = m_x(\infty)$ and $b_x = m_x(\infty) - m_x(1)$ would serve as valid/appropriate choices for the reference values a_x and scaling factors b_x,

$$m_x(n) = m_x(\infty) + \frac{m_x(1) - m_x(\infty)}{n^{1/3}}. \tag{4b}$$

Such a choice may look obvious at first sight. It is not forcing, however, and it takes verification. In any case, one needs to consider independently the spin and orbital contributions ($x = S, L$) to the magnetic moments of the Fe_n^+, Co_n^+, and Ni_n^+ clusters. This takes to verify six sets of parameters (a_x, b_x, y_x), which gives 18 values in total.

Figs. 4(a) and 4(b) visualize an attempt to compare the recorded spin and orbital magnetic moments of the Fe_n^+, Co_n^+, and Ni_n^+ clusters to conceivable scaling laws. The x-axes of diagrams are chosen as $n^{-1/3}$ (namely, $y_x = -1/3$) which makes any accordingly scaling data set resemble a straight line. Note that alternative scaling laws may be visualized by nonlinear curves as was done, e.g., between the same asymptotes in Fig. 4(a) by dashed lines for the case of $y_S = -1$ (which corresponds to a scaling "per cluster volume").

A. Spin moments

It is gratifying to realize that the recorded cluster data of spin magnetic moments (data points in Fig. 4(a)) come close to the conceived scaling law in the three cases of Fe_n^+ (blue diamonds), Co_n^+ (green circles), and Ni_n^+ (red triangles). In particular, the scaling "per diameter" ($y_S = -1/3$) reproduces the experimental data on spin contributions quite well. It would be inappropriate to consider an alternative scaling law "per cluster volume" ($y_S = -1$). An intermediate case of scaling "per surface area" ($y_S = -1/2$) is obviously not suitable either.

We conclude from this scaling law that the average spin magnetic moment per atom seems to follow the surface area of the cluster (normalized to the cluster volume). In a first try of an explanation, we can follow the argumentation that rationalizes the enhanced spin magnetic moment at surfaces and of thin films. The reduced coordination number at surfaces leads to a stronger localization of the electron wave function and thus to a narrower band width which in turn leads to a higher density of states at surface atoms.[42,84,89] This leads to an enhanced spin magnetic moment at surfaces. As our measurement averages over all coordination sites (surface and volume), enhanced spin moments at surface sites will lead to an enhancement with respect to the bulk of the average spin magnetic moment per atom in clusters. This leads to a scaling by 1 over area per volume which appears as $n^{-1/3}$, as observed. This might explain why the surface area is important. Individual size effects—few of which we find in our present data—should be superimposed onto the scaling law. If the investigated size range was to be extended towards larger and/or smaller clusters, the scaling trend should become more pronounced.

It remains to discuss whether the choice of the spin reference value $a_S = m_S(\infty)$ and of the spin scaling factor $b_x = m_S(1) - m_S(\infty)$ according to Eq. (4b) is appropriate. The onset of complex (multi-domain) magnetic phases, which are characteristic for the bulk sample, is far beyond the size of the clusters investigated in this and other studies. Thus, single domain bulk spin moments might seem a more appropriate choice for the spin reference value a_S. However, the cited values (cf. Table II.) stem from bulk XMCD studies which were conducted at saturation field strength where the magnetization of all domains was flipped into easy axis alignment with respect to the applied external field. Under such conditions,

the recording of bulk magnetization values may yield single domain like values which in turn suite for comparison to super paramagnetic clusters.

For the atom, the increased spin moment is not due to unpaired 4s electrons but a consequence of a completely filled 4s orbital, which causes an additional hole in the 3d shell. This feature is already absent if one goes to a diatomic molecule. Thus, for different reasons, surface and isolated atoms have an increased spin moment, and the difference between large clusters and the bulk is not too large. Note that in the case of nickel, the solid line seems to be too low. Maybe this is caused by a particularly small value of the spin moment per atom for the bulk.

B. Orbital moments

There are remarkably different findings in the cases of the orbital magnetic moments (Fig. 4(b)) of Fe_n^+ (blue diamonds), Co_n^+ (green circles), and Ni_n^+ (red triangles). For sure, they are not explained by a "per diameter" scaling as given by Eq. (4b) (dashed lines in Fig. 4(b)). The found cluster values are quite small (<0.6 μ_B/atom). They range close to the quenched asymptotic bulk values and they are far below the atomic values. Those unquenched atomic orbital moments (of first order or primary nature) arise exclusively from orbitally degenerate ground states (where both clockwise and counterclockwise rotations are equally possible). Clustering lifts symmetry related degeneracies, and arbitrary degeneracies are unlikely—those would be lifted by a Jahn-Teller distortion. Henceforth, primary orbital moments of clusters necessarily vanish, they are completely quenched. If one "switches on" the spin-orbit coupling for a system of non-degenerate orbitals, small orbital moments are induced by mixing in exited states. We like to call those orbital moments "second order" or "secondary." The same mechanism is responsible for the shift of the g value in transition metal complexes, which is well known to result from an interplay of spin-orbit coupling and the local environment (crystal field). It is therefore reasonable to assume that coordination geometries and orbital occupancies interdepend. A change from bulk to surface coordination thus changes orbital occupancies in the affected atom(s). We therefore state that the fraction of surface atoms may serve as a measure for the cluster size related change in orbital moments, in accordance with Eq. (4a), $y_L = -1/3$. The choice of reference value is obvious, as well, $a_L = m_L(\infty)$. As of the orbital scaling factor b_L, an *a priori* choice is not possible. Instead, we take the recorded $m_L(n)$ values to perform a linear fit (of b_L) to Eq. (4a). The results of such fits are indicated in Fig. 4(b) by solid lines which quite convincingly reproduce the observed orbital values. It would be decisive to obtain experimental data for the clusters n = 2 and n = 3. Predicted values for the case of n = 2 are indicated in the figure (Fig. 4(b), solid symbols).

Surface layers of transition metals are known to show an enhanced orbital moment compared to the bulk phase.[17] This has been attributed before to the fact that atoms have a lower coordination number than bulk atoms and the 3d states are more localized than in the solid.[13,90,91] Hence, surface atoms are said to retain more angular orbital momentum than their bulk counterparts. Our present findings on isolated clusters are fully in line with this line of arguments. The orbital moment per transition metal atom should thus follow the ratio of surface atoms-to-bulk atoms (Eq. (4a)). It might follow that the general geometry of the clusters influences the orbital moment more strongly than the spin magnetic moment, i.e., the coordination environment, number of nearest neighbors, and bond lengths. Exceptionally, high or low orbital magnetic moments may appear for certain cluster geometries which have an open structure (high orbital magnetic moment) or a high symmetry (small orbital magnetic moment). In the case of the orbital magnetic moment, one might see a significant change if the geometrical motif changes, e.g., from icosahedral to bulk like. Future experiments might cover an extended size range to elucidate such a transition in crystalline structure.

C. Validation of scaling laws

It is a general question of concern whether a continuous scaling of magnetic cluster properties amongst atomic and bulk values is to be expected in the first place. Discontinuous (phase) transitions are well conceivable. At present, we are able to phrase a "robust" finding of the present study *without* stating any scaling: spin and orbit contributions of iron, cobalt, and nickel clusters comprising 10–20 atoms are closer to bulk than to atomic values. The relative quenching of orbital moments in clusters is higher than that of the spin moments. A definite interpretation of the found scaling laws is pending and will need further support from theory.

Current interpretation discusses spin and orbital moments of ground state atomic configurations, $4s^2 3d^x$ as asymptotes of scaling laws. It is conceivable to consider instead the spin and orbital moments of metastable $4s^1 3d^{x+1}$ atomic configurations which closer resemble bulk type bonding. When doing so, the found spin moment scaling would diminish. Our conclusions on two types of orbital moments would not alter. We thus refrain from elaborating further into this direction.

V. SUMMARY AND OUTLOOK

We have investigated the spin and orbital magnetic moments of small iron (Fe_n^+, $7 \le n \le 18$), cobalt (Co_n^+, $8 \le n \le 17, 19, 22$), and nickel (Ni_n^+, $7 \le n \le 17$) clusters. In all cases, we have investigated the spin magnetic moments, the orbital magnetic moments, and the total magnetic moments that are enhanced with respect to the corresponding values of the bulk material and quenched with respect to the atomic values.

The current spin magnetic moments by XMCD of Fe_n^+ are lower by 10% than those of a recent, independent XMCD experiment.[25] The current spin magnetic moments by XMCD of Co_n^+ are lower by 10% than previous XMCD values.[26] The current spin magnetic moments by XMCD of Ni_n^+ are larger by 10%–20% than previous XMCD values.[25] In all three cases, deviations are within combined uncertainties or slightly beyond. The orbital magnetic moments of Fe_n^+, Co_n^+, and Ni_n^+ are smaller by a factor of 2.5–20 than the spin magnetic moments, current and previous XMCD data well agreeing. The current investigation thus provides for an independent

verification of the spin and orbital contributions of magnetic moments in cationic iron, cobalt, and nickel clusters by the XMCD technique, and it extends the size ranges of studied cobalt and nickel clusters with respect to the previous studies.

The total magnetic moments of Fe_n^+ and Co_n^+ clusters by XMCD range above and below those of Fe_n and Co_n clusters by various Stern-Gerlach studies. The total magnetic moments of Ni_n^+ clusters by XMCD range above those of Ni_n clusters by three Stern-Gerlach studies. In all three cases, the XMCD values of spin magnetic moments come closer to the recorded total magnetic moments by Stern-Gerlach. Reduced moments at n = 13 in iron coincide in XMCD and SG studies. The reduced total magnetic moment of Ni_{14}^+ by XMCD stays in contrast to a reduced magnetic moment in Ni_{13}^+ by SG. A balancing of unpaired d-electrons versus vacancies suggests that cluster charge (cationic or neutral) matters in small nickel clusters, while it is of less influence in large iron clusters.

Contemporary DFT calculations conclude on spin magnetic moments of Fe_n^+ ($7 \le n \le 20$) in line with the present XMCD values but low with respect to previous XMCD data. Computations of Co_n^+ ($n \le 30$) and of Ni_n^+ ($n \le 30$) seem to underestimate the spin magnetic moments by XMCD of the present study and of the previous studies. It is possible that conceptual problems prevail in approximate exchange-correlation functionals. There are few predictions of orbital magnetic moments through perturbative spin orbit coupling (SOC) calculations which yield reasonable values in cases of small iron and nickel clusters. It is emphasized that broken symmetry DFT calculations are desperately needed in order to verify possible or even likely antiferromagnetic couplings. Furthermore, our present findings call for verification through future *ab initio* calculations that take spin orbit coupling explicitly into account.

We devise scaling laws that interpret the recorded spin and orbital magnetic moments in terms of surface effects which leads to $n^{-1/3}$ size dependencies in both cases. The spin magnetic moments interpolate between atomic and bulk values. The orbital magnetic moments interpolate between dimer and bulk values, with the atomic value exempt. We find a rationalization by recalling the very nature of "primary" atomic orbital moments and "secondary" spin-orbit-coupling induced orbital moments in clusters, the former being quenched in aggregates through loss of symmetry and concomitant loss of orbital degeneracies.

The presented results and compilation of the actual state of research in spin and orbital contributions to total magnetic moments in isolated clusters of ferromagnetic 3d elements provide a solid base for future investigations: an advanced computational treatment of induced orbital magnetic moments; the elucidation by future experiments of the interplay of spin state in clusters and adsorbates on clusters; the unravelling of electronic and magnetic couplings of bulk surfaces to deposited clusters; the determination of intrinsic magnetism in nonstoichiometric sub-oxides in clusters of ferromagnetic metals; the unravelling of spin and orbital contributions of magnetic moments in alloy clusters; and the systematic investigation of magnetic anisotropy and its influence on sum rule analysis.

ACKNOWLEDGMENTS

This work has been supported by the Deutsche Forschungsgemeinschaft (No. NIE325/10-1) and in the framework of the Transregional Collaborative Research Center No. SFB/TRR 88 "**3MET.de**" and of the Collaborative Research Center No. SFB 668. Further support (W.W.) arose through the BMBF Project No. 05K10HRB. We are grateful for valuable discussions with Kai Fauth (University of Würzburg), Paul Bechthold, and Stefan Bluegel (Forschungszentrum Jülich). We also thank Patrick Hofmann (Brandenburg University of Technology Cottbus), Stefan Krause, and Ruslan Ovsyannikov (Helmholtz Zentrum Berlin, HZB) for assistance at the beamline UE52-PGM at BESSY II, and we thank the HZB for allocation of synchrotron radiation beam time.

APPENDIX A: ON GYROMAGNETIC RATIOS

The magneto-mechanical ratio g′ can be deduced from gyromagnetic experiments by the Einstein-de Haas effect[92] (rotation induced by change of the magnetization). g′ differs from the g factor determined by Ferromagnetic resonance (FMR) experiments. The definition of g′ includes J_{tot} and thus a contribution of the orbital angular momentum J_{orbit} (L). The definition of g, on the other hand, only includes the spin angular momentum J_{spin}(= S).[93,94] The value of the free electron, i.e., the spin only value, is equal to two for g and g′ (neglecting QED corrections). However, the deviation due to the orbital angular momentum results in g > 2 and g′ < 2,

$$g' = \frac{2m_e}{e}\frac{M}{J_{tot}} = \frac{2m_e}{e}\frac{M}{J_{spin}+J_{orbit}},$$

$$g = \frac{2m_e}{e}\frac{M}{J_{spin}},$$

$$\frac{g'}{g} = \frac{J_{spin}}{J_{spin}+J_{orbit}} = \frac{S}{S+L}.$$

APPENDIX B: FROM A TAYLOR EXPANSION TO SCALING LAWS

Any steady differentiable function $f(x)$ may be defined through a Taylor expansion around a given point x_0,

$$f(x) = f(x_0) + \sum_{n=1}^{\infty}\frac{1}{n!}\left(\left.\frac{df(x)}{dx^n}\right|_{x=x_0}\right)(x-x_0)^n. \quad \text{(B1)}$$

Regarding a cluster size dependent entity $m(n)$ as a smoothly varying function of a continuous variable n, one may conceive an according expansion of $m(n)$ by orders of j and around a cluster size n_0,

$$m(n) = m(n_0) + \sum_{j=1}^{\infty}\frac{1}{j!}\left(\left.\frac{dm(n)}{dn^j}\right|_{n=n_0}\right)(n-n_0)^j. \quad \text{(B2)}$$

Physical effects often cause cluster size dependencies to run by some power y of n, $m(n) \sim const. + n^y$ (cf. Table II). Such simple cases justify a truncation of the Taylor expansion at $j_{max} = y$ if $y > 0$.

In cases of inverse power dependencies, $y < 0$, however, an according Taylor expansion would require exceedingly

many terms in order to achieve an accurate description of $m(n)$. It becomes advantageous to invoke a more appropriate transformation of the independent variable than the prior mapping $x \leftrightarrow n$. Instead, it is conceivable to apply $x \leftrightarrow n^y = \frac{1}{n^{|y|}}$. This yields

$$m(n) = m(n_0) + \sum_{j=1}^{\infty} \frac{1}{j!} \left(\left. \frac{dm(n)}{d(n^y)^j} \right|_{n=n_0} \right) (n^y - {n_0}^y)^j. \tag{B3}$$

Approximation to first order, $j_{max} = 1$, leads towards formulation of known scaling laws, while choice of $n_0 = \infty$ helps to simplify

$$m(n) = m(\infty) + \left(\left. \frac{dm(n)}{d(n^y)} \right|_{n=\infty} \right) n^y = m(\infty) + c_\infty n^y. \tag{B4}$$

The significance of $m(\infty) = m_{bulk}$ is obvious. The slope coefficient c_∞ takes interpretation. As of now, it is defined as a local entity at $n = \infty$. In case of the above first order approximation by a single power term n^y, it is constant and does not vary by n. This allows to interpret

$$c_\infty = \left. \frac{dm(n)}{d(n^y)} \right|_{n=\infty} = \frac{\Delta m(n)}{\Delta(n^y)} = -(m(\infty) - m(1)). \tag{B5}$$

Note that the denominator $\Delta(n^y)$ has conveniently reduced with $y < 0$ and choice of interval $\Delta n = [\infty, 1]$ to $\Delta(n^y) = -1$. The resulting scaling law then reads (with $m(1) = m_{atom}$)

$$m(n) = m_{bulk} - \frac{m_{bulk} - m_{atom}}{n^{|y|}}. \tag{B6}$$

Alternate choices of interval Δn for evaluation of slope coefficient c_{n_0} would lead to according formulas, which would be slightly more complicated. E.g., a choice of $\Delta n = [\infty, 2]$ would yield

$$m(n) = m_{bulk} - 2^{|y|} \frac{m_{bulk} - m(2)}{n^{|y|}}. \tag{B7}$$

With the prior cluster surface to volume arguments $y = -1/3$, and the scaling law of spin contributions to cluster magnetic moments ($\Delta n = [\infty, 1]$) becomes

$$m_S(n) = m_{S,bulk} - \frac{m_{S,bulk} - m_{S,atom}}{\sqrt[3]{n}}. \tag{B8}$$

Accordingly, the scaling law for orbital contributions to cluster magnetic moments within the reduced size interval ($\Delta n = [\infty, 2]$) becomes

$$m_L(n) = m_{L,bulk} - \frac{m_{L,bulk} - m_{L,dimer}}{\sqrt[3]{n/2}}. \tag{B9}$$

Both laws may be combined to a joint law for total magnetic moments,

$$m_{tot}(n) = m_S(n) + m_L(n) = m_{tot,bulk} - \frac{(m_{S,bulk} - m_{S,atom}) + \sqrt[3]{2}\,(m_{L,bulk} - m_{L,dimer})}{\sqrt[3]{n}}. \tag{B10}$$

[1]Y.-W. Jun, J.-W. Seo, and A. Cheon, Acc. Chem. Res. **41**, 179 (2008).
[2]H. Haberland, *Clusters of Atoms and Molecules* (Springer, 1994).
[3]K. H. Meiwes-Broer, *Metal Clusters at Surfaces* (Springer, 2000).
[4]L. Glaser, K. Chen, S. Fiedler, M. Wellhöfer, W. Wurth, and M. Martins, Phys. Rev. B **86**, 075435 (2012).
[5]W. Wurth and M. Martins, Chem. Phys. Solid Surf. **12**, 471 (2007).
[6]E. Antonsson, H. Bresch, R. Lewinski, B. Wassermann, T. Leisner, C. Graf, B. Langer, and E. Rühl, Chem. Phys. Lett. **559**, 1 (2013).
[7]I. M. L. Billas, A. Châtelain, and W. A. de Heer, Science **265**, 1682 (1994).
[8]Y. Z. Wu, B. Sinkovic, C. Won, J. Zhu, Y. Zhao, and Z. Q. Qiu, Phys. Rev. B **85**, 134436 (2012).
[9]M. B. Knickelbein, J. Chem. Phys. **116**, 9703 (2002).
[10]M. B. Knickelbein, J. Chem. Phys. **115**, 1983 (2001).
[11]S. E. Apsel, J. W. Emmert, J. Deng, and L. A. Bloomfield, Phys. Rev. Lett. **76**, 1441 (1996).
[12]J. A. Alonso, Chem. Rev. **100**, 637 (2000).
[13]J. Stöhr, J. Electron Spectrosc. Relat. Phenom. **75**, 253 (1995).
[14]C. T. Chen, Y. U. Idzerda, H. J. Lin, N. V. Smith, G. Meigs, E. Chaban, G. H. Ho, E. Pellegrin, and F. Sette, Phys. Rev. Lett. **75**, 152 (1995).
[15]G. Schütz, W. Wagner, W. Wilhelm, P. Kienle, R. Zeller, R. Frahm, and G. Materlik, Phys. Rev. Lett. **58**, 737 (1987).
[16]P. Gambardella, S. Rusponi, M. Veronese, S. S. Dhesi, C. Grazioli, A. Dallmeyer, I. Cabria, R. Zeller, P. H. Dederichs, K. Kern, C. Carbone, and H. Brune, Science **300**, 1130 (2003).
[17]S. S. Dhesi, H. A. Dürr, G. van der Laan, E. Dudzik, and N. B. Brookes, Phys. Rev. B **60**, 12852 (1999).
[18]P. Gambardella, A. Dallmeyer, K. Maiti, M. C. Malagoli, W. Eberhardt, K. Kern, and C. Carbone, Nature **416**, 301 (2002).
[19]J. Bansmann, A. Kleibert, M. Getzlaff, A. F. Rodriguez, F. Nolting, C. Boeglin, and K.-H. Meiwes-Broer, Phys. Status Solidi B **247**, 1152 (2010).
[20]J. T. Lau, A. Föhlisch, R. Nietubyč, M. Reif, and W. Wurth, Phys. Rev. Lett. **89**, 057201 (2002).
[21]K. Chen, S. Fiedler, I. Baev, T. Beeck, W. Wurth, and M. Martins, New J. Phys. **14**, 123005 (2012).
[22]H. Brune and P. Gambardella, Surf. Sci. **603**, 1812 (2009).
[23]T. Eelbo, M. Waśniowska, P. Thakur, M. Gyamfi, B. Sachs, T. O. Wehling, S. Forti, U. Starke, C. Tieg, A. I. Lichtenstein, and R. Wiesendanger, Phys. Rev. Lett. **110**, 136804 (2013).
[24]S. Peredkov, M. Neeb, W. Eberhardt, J. Meyer, M. Tombers, H. Kampschulte, and G. Niedner-Schatteburg, Phys. Rev. Lett. **107**, 233401 (2011).
[25]M. Niemeyer, K. Hirsch, V. Zamudio-Bayer, A. Langenberg, M. Vogel, M. Kossick, C. Ebrecht, K. Egashira, A. Terasaki, T. Möller, B. v. Issendorff, and J. T. Lau, Phys. Rev. Lett. **108**, 057201 (2012).
[26]A. Langenberg, K. Hirsch, A. Lawicki, V. Zamudio-Bayer, M. Niemeyer, P. Chmiela, B. Langbehn, A. Terasaki, B. V. Issendorff, and J. T. Lau, Phys. Rev. B **90**, 184420 (2014).
[27]S. Peredkov, A. Savci, S. Peters, M. Neeb, W. Eberhardt, H. Kampschulte, J. Meyer, M. Tombers, B. Hofferberth, F. Menges, and G. Niedner-Schatteburg, J. Electron Spectrosc. Relat. Phenom. **184**, 113 (2011).
[28]C. Berg, T. Schindler, G. Niedner-Schatteburg, and V. E. Bondybey, J. Chem. Phys. **102**, 4870 (1995).
[29]S. Maruyama, L. R. Anderson, and R. E. Smalley, Rev. Sci. Instrum. **61**, 3686 (1990).
[30]D. Proch and T. Trickl, Rev. Sci. Instrum. **60**, 713 (1989).
[31]P. Carra, B. T. Thole, M. Altarelli, and X. Wang, Phys. Rev. Lett. **70**, 694 (1993).
[32]B. T. Thole, P. Carra, F. Sette, and G. Vanderlaan, Phys. Rev. Lett. **68**, 1943 (1992).
[33]P. G. Alvarado-Leyva, F. Aguilera-Granja, L. C. Balbas, and A. Vega, Phys. Chem. Chem. Phys. **15**, 14458 (2013).
[34]O. Sipr and H. Ebert, Phys. Rev. B **72**, 134406 (2005).
[35]R. Wu and A. J. Freeman, Phys. Rev. Lett. **73**, 1994 (1994).
[36]P. Srivastava, F. Wilhelm, A. Ney, M. Farle, H. Wende, N. Haack, G. Ceballos, and K. Baberschke, Phys. Rev. B **58**, 5701 (1998).
[37]P. Srivastava, N. Haack, H. Wende, R. Chauvistré, and K. Baberschke, Phys. Rev. B **56**, R4398 (1997).
[38]N. W. Ashcroft and N. D. Mermin, *Festkörperphysik*, 4th ed. (Oldenbourg Verlag, München, 2013).
[39]J. Stöhr and H. C. Siegmann, *Magnetism: From Fundamentals to Nanoscale Dynamics*, Springer Series in Solid-State Sciences Vol. 152 (Springer, 2006).
[40]W. C. Elmore, Phys. Rev. **54**, 1092 (1938).
[41]S. N. Khanna and S. Linderoth, Phys. Rev. Lett. **67**, 742 (1991).
[42]H. Brune and P. Gambardella, *Atomic and molecular magnets on surfaces* (CRC Press, 2014), p. 447.
[43]O. Sipr, J. Minar, and H. Ebert, Europhys. Lett. **87**, 67007 (2009).
[44]J. Stöhr and H. König, Phys. Rev. Lett. **75**, 3748 (1995).
[45]C. G. Stefanita, *Magnetism: Basics and Applications* (Springer, 2012).
[46]J. P. Bucher, D. C. Douglass, and L. A. Bloomfield, Phys. Rev. Lett. **66**, 3052 (1991).

[47]B. V. Reddy, S. K. Nayak, S. N. Khanna, B. K. Rao, and P. Jena, J. Phys. Chem. A **102**, 1748 (1998).
[48]G. van der Laan, J. Synchrotron Radiat. **6**, 694 (1999).
[49]C. T. Chen, N. V. Smith, and F. Sette, Phys. Rev. B **43**, 6785 (1991).
[50]J. Vogel and M. Sacchi, Phys. Rev. B **49**, 3230 (1994).
[51]X. Xu, S. Yin, R. Moro, A. Liang, J. Bowlan, and W. A. de Heer, Phys. Rev. Lett. **107**, 057203 (2011).
[52]F. W. Payne, W. Jiang, J. W. Emmert, J. Deng, and L. A. Bloomfield, Phys. Rev. B **75**, 094431 (2007).
[53]M. B. Knickelbein, J. Chem. Phys. **125**, 044308 (2006).
[54]X. S. Xu, S. Y. Yin, R. Moro, and W. A. de Heer, Phys. Rev. Lett. **95**, 237209 (2005).
[55]M. B. Knickelbein, Chem. Phys. Lett. **353**, 221 (2002).
[56]P. J. Jensen and K. H. Bennemann, Z. Phys. D: At., Mol. Clusters **35**, 273 (1995).
[57]R. A. Guirado-López, J. Dorantes-Dávila, and G. M. Pastor, Phys. Rev. Lett. **90**, 226402 (2003).
[58]G. L. Gutsev, C. A. Weatherford, P. Jena, E. Johnson, and B. R. Ramachandran, J. Phys. Chem. A **116**, 10218 (2012).
[59]A. N. Andriotis and M. Menon, Phys. Rev. B **57**, 10069 (1998).
[60]C. Köhler, G. Seifert, and T. Frauenheim, Chem. Phys. **309**, 23 (2005).
[61]O. Diéguez, M. Alemany, C. Rey, P. Ordejón, and L. Gallego, Phys. Rev. B **63**, 205407 (2001).
[62]P. Bobadova-Parvanova, K. Jackson, S. Srinivas, M. Horoi, C. Köhler, and G. Seifert, J. Chem. Phys. **116**, 3576 (2002).
[63]K. Takahashi, S. Isobe, and S. Ohnuki, Appl. Phys. Lett. **102**, 113108 (2013).
[64]J. Guevara, F. Parisi, A. M. Llois, and M. Weissmann, Phys. Rev. B **55**, 13283 (1997).
[65]D. Roy, R. Robles, and S. Khanna, J. Chem. Phys. **132**, 194305 (2010).
[66]H. K. Yuan, H. Chen, A. L. Kuang, C. L. Tian, and J. Z. Wang, J. Chem. Phys. **139**, 034314 (2013).
[67]G. Guzmán-Ramírez, P. Salvador, J. Robles, A. Vega, and F. Aguilera-Granja, Theor. Chem. Acc. **132**, 1 (2012).
[68]G. L. Gutsev, C. W. Weatherford, K. G. Belay, B. R. Ramachandran, and P. Jena, J. Chem. Phys. **138**, 164303 (2013).
[69]M. Pérez, F. Muñoz, J. Mejía-López, and G. Martínez, J. Nanopart. Res. **14**, 1 (2012).
[70]S. Datta, M. Kabir, S. Ganguly, B. Sanyal, T. Saha-Dasgupta, and A. Mookerjee, Phys. Rev. B **76**, 014429 (2007).
[71]J. Rodríguez-López, F. Aguilera-Granja, K. Michaelian, and A. Vega, Phys. Rev. B **67**, 174413 (2003).
[72]Q.-M. Ma, Z. Xie, J. Wang, Y. Liu, and Y.-C. Li, Phys. Lett. A **358**, 289 (2006).
[73]C. Dong and X. Gong, Phys. Rev. B **78**, 020409 (2008).
[74]F. Aguilera-Granja, A. Vega, and L. C. Balbás, Chem. Phys. **415**, 106 (2013).
[75]J. H. Mokkath, J. Magn. Magn. Mater. **349**, 109 (2014).
[76]G. Martínez, E. Tangarife, M. Pérez, and J. Mejía-López, J. Phys.: Condens. Matter **25**, 216003 (2013).
[77]W. Song, W.-C. Lu, C. Z. Wang, and K. M. Ho, Comput. Theor. Chem. **978**, 41 (2011).
[78]F. Aguilera-Granja, S. Bouarab, M. López, A. Vega, J. Montejano-Carrizales, M. Iniguez, and J. Alonso, Phys. Rev. B **57**, 12469 (1998).
[79]F. Reuse and S. Khanna, Chem. Phys. Lett. **234**, 77 (1995).
[80]Q. Lu, Q. Luo, L. Chen, and J. Wan, Eur. Phys. J. D **61**, 389 (2011).
[81]M. Wu, A. K. Kandalam, G. L. Gutsev, and P. Jena, Phys. Rev. B **86**, 174410 (2012).
[82]E. M. Kessler, S. Schmitt, and C. van Wüllen, J. Chem. Phys. **139**, 184110 (2013).
[83]C. van Wüllen, J. Phys. Chem. A **113**, 11535 (2009).
[84]C. A. F. Vaz, J. A. C. Bland, and G. Lauhoff, Rep. Prog. Phys. **71**, 056501 (2008).
[85]I. Rips and J. Jortner, J. Chem. Phys. **97**, 536 (1992).
[86]H. Haberland, K. Kleinermanns, and F. Träger, *Lehrbuch der Experimentalphysik Band 5: Gase, Nanosysteme, Flüssigkeiten* (Walter de Gruyter, 2006), p. 819.
[87]P. Atkins and J. de Paula, *Elements of Physical Chemistry*, 4th ed. (W. H. Freeman and Company, Oxford, 2005), p. 9.
[88]It might seem confusing at first sight to define continuously varying cluster entities (diameter, volume) by relating them to a discrete number of building blocks (atoms). This is straightforward and valid to a very good approximation as long as dense packing dominates. Sometimes, such approximation is labeled as a "liquid drop model."
[89]S. Blügel, *Lecture Notes Magnetism Goes Nano: Electron Correlations, Spin Transport, Molecular Magnetism* (Forschungszentrum Jülich in der Helmholtz-Gemeinschaft, 2005).
[90]J. Stöhr, J. Magn. Magn. Mater. **200**, 470 (1999).
[91]M. Tischer, O. Hjortstam, D. Arvanitis, J. Hunter Dunn, F. May, K. Baberschke, J. Trygg, J. M. Wills, B. Johansson, and O. Eriksson, Phys. Rev. Lett. **75**, 1602 (1995).
[92]A. Einstein and W. J. de Haas, Verhandlungen der Deutschen Physikalischen Gesellschaft **17**, 152 (1915).
[93]C. Kittel, Phys. Rev. **76**, 743 (1949).
[94]T. M. Wallis, J. Moreland, and P. Kabos, Appl. Phys. Lett. **89**, 122502 (2006).
[95]G. G. Scott and H. W. Sturner, Phys. Rev. **184**, 490 (1969).
[96]G. G. Scott, Phys. Rev. **148**, 525 (1966).
[97]G. G. Scott and R. A. Reck, Phys. Rev. B **8**, 233 (1973).
[98]G. Nave, S. Johansson, R. C. M. Learner, A. P. Thorne, and J. W. Brault, Astrophys. J., Suppl. Ser. **94**, 221 (1994).
[99]NIST ASD Team, NIST Atomic Spectra Database (ver. 5.1) (National Institute of Standards and Technology, Gaithersburg, MD, 2013), available online at http://physics.nist.gov/asd.
[100]G. Nave and S. Johansson, Astrophys. J., Suppl. Ser. **204**, 1 (2013).
[101]J. Sugar and C. Corliss, J. Phys. Chem. Ref. Data **14** Supplement 2, 1 (1985).
[102]J. C. Pickering, A. J. J. Raassen, P. H. M. Uylings, and S. Johansson, Astrophys. J., Suppl. Ser. **117**, 216 (1998).
[103]L. Ulf, W. B. James, and P. T. Anne, Phys. Scr. **47**, 628 (1993).
[104]A. Kohn, F. Weigend, and R. Ahlrichs, Phys. Chem. Chem. Phys. **3**, 711 (2001).
[105]T. Bachels and R. Schäfer, Chem. Phys. Lett. **324**, 365 (2000).
[106]F. Baletto and R. Ferrando, Rev. Mod. Phys. **77**, 371 (2005).
[107]G. Wrigge, M. A. Hoffmann, and B. v. Issendorff, Phys. Rev. A **65**, 063201 (2002).
[108]M. B. Knickelbein and S. Yang, J. Chem. Phys. **93**, 5760 (1990).
[109]G. Wrigge, M. Astruc Hoffmann, B. Issendorff, and H. Haberland, Eur. Phys. J. D **24**, 23 (2003).
[110]W. A. de Heer, Rev. Mod. Phys. **65**, 611 (1993).
[111]M. M. Alvarez, J. T. Khoury, T. G. Schaaff, M. N. Shafigullin, I. Vezmar, and R. L. Whetten, J. Phys. Chem. B **101**, 3706 (1997).
[112]W. A. de Heer, in *Metal Clusters at Surfaces*, edited by K.-H. Meiwes-Broer (Springer, 2000).
[113]C. Brechignac, M. Broyer, P. Cahuzac, G. Delacretaz, P. Labastie, and L. Wöste, Chem. Phys. Lett. **120**, 559 (1985).
[114]C. Bréchignac, M. Broyer, P. Cahuzac, G. Delacretaz, P. Labastie, J. P. Wolf, and L. Wöste, Phys. Rev. Lett. **60**, 275 (1988).
[115]G. M. Pastor and K. H. Bennemann, in *Clusters of Atoms and Molecules*, edited by H. Haberland (Springer, 1994).
[116]M. R. Harrison and P. P. Edwards, in *The Metallic and Non-Metallic States of Matter*, edited by P. P. Edwards and C. N. R. Rao (Francis & Taylor, London, 1985).
[117]M. Getzlaff, *Fundamentals of Magnetism* (Springer, 2008).
[118]See supplementary material at http://dx.doi.org/10.1063/1.4929482 for a comparison of experimental and theoretical spin magnetic moments in μ_B/atom (Table S3a). In Table S3b, we show a comparison of experimental orbital magnetic moments in μ_B/atom. In Figure S1, we show spin and orbital magnetic moments of size selected clusters in comparison to conceivable trends that would interpolate between bulk metals and cationic atoms. In Figure S2, we show a comparison of spin and orbital magnetic moments for Fe_n^+, Co_n^+, and Ni_n^+ clusters from this study and data obtained by Lau *et al.* In Figure S3, we show theoretical data on the spin magnetic moments of Fe clusters. In Figure S4, we show theoretical data on the spin magnetic moments of Co clusters. In Figure S5, we show theoretical data on the spin magnetic moments of Ni clusters.